Journal of Magnetic Resonance **152,** 87–94 (2001)
doi:10.1006/jmre.2001.2387, available online at http://www.idealibrary.com on IDEAL®

Rheology of Blood by NMR

Song-I Han,* Oliver Marseille,† Christa Gehlen,* and Bernhard Blümich*

*Institut für Technische Chemie und Makromolekulare Chemie, Rheinisch-Westfälische Technische Hochschule, Worringerweg 1, 52074 Aachen, Germany; and †Helmholtz Institut für Biomedizinische Technik, Rheinisch-Westfälische Technische Hochschule, Pauwelstrasse 30, 52074 Aachen, Germany

Received January 8, 2001; revised June 7, 2001

Pipe flow of blood in tubes of 1 and 7 mm inner diameter, respectively, was investigated employing two-dimensional NMR velocity imaging and PFG propagator measurements at different Reynolds numbers between 10 and 3500. The results are compared to flow of a water/glycerol mixture of matching viscosity under identical conditions. The transition from laminar to turbulent flow is observed by both a flattening of the velocity profile and a change of the propagator shape. For blood flow this transition is found to be shifted toward higher Reynolds numbers as compared to the transition of the water/glycerol mixture. This observation is in agreement with predictions from hydraulic measurements and is a consequence of the non-Newtonian flow characteristics of blood as a suspension of erythrocytes and plasma. Likewise, a deviation from the laminar flow condition is observed for blood at low Reynolds numbers between 10 and 100. This phenomenon is unknown for Newtonian liquids and is explained by the onset of a geometrical arrangement of the erythrocytes, the so-called rouleaux effect.

Key Words: **blood; suspension; velocity imaging; turbulent flow; propagator.**

INTRODUCTION

Blood is a complex heterogeneous suspension with small cellular particles finely distributed in blood plasma. Red blood cells (erythrocytes) comprise the majority of these particles. The specific rheological behavior of blood can mainly be attributed to these erythrocytes. The hematocrit value, which measures the volume fraction of red blood cells, amounts to 40–50% and thus exceeds by far the solid volume fraction of any technically used suspension with flowing behaviour. Many studies exist dealing with the behavior of blood flow in the human body (*1–3*), however, few and controversial results about the transition point from laminar to turbulent flow and the turbulence behavior itself of blood have been presented (*4–6*). The particular interest in flow properties of blood under very high and low shear rates was induced by the development ofminiaturized micro blood pumps, where unphysiologically high flow velocities occur locally (*7, 8*). We have examined pipe flow as the simplest model case of blood flow.

Under laminar conditions the Newtonian fluid moves smoothly in concentric layers or *laminae*. The shear stress is a linear function of the radial position r in the pipe, resulting in a parabolic velocity profile $v(r)$:

$$v(r) = \frac{\Delta p \cdot r_0^2}{4 \cdot \eta \cdot l} \cdot \left(1 - \frac{r^2}{r_0^2}\right) = v_{max} \cdot \left(1 - \frac{r^2}{r_0^2}\right). \quad [1]$$

Here η is the dynamic viscosity, Δp is the pressure drop along the flow direction within a pipe length of l, and r_0 is the radius of the pipe. This relationship leads to the following proportionalities of the volume flow rate $\dot{V}$, which is called the Hagen–Poiseuille law:

$$\dot{V} = \frac{\pi \cdot r_0^4 \cdot \Delta p}{8 \cdot \eta \cdot l}. \quad [2]$$

Laminar flow is present at low velocities. Turbulent flow with much more complex behavior occurs, starting from a characteristic value for high flow rates, called the critical Reynolds (Re) number Re_c. This transition is governed by a combination of the fluid density ρ, dynamic viscosity η, the average flow velocity $\bar{v}$, and the tube diameter d and their dimensionless combination is known as the Reynolds number, expressed mathematically as

$$Re = \frac{\rho \cdot \bar{v} \cdot d}{\eta}. \quad [3]$$

The Reynolds number can be understood as the ratio of inertial force and viscous force and characterizes the friction effect (*9*).

Turbulent flow is characterized by an unsteady and irregular eddying motion, which is superimposed on the mean flow. At a fixed point in a turbulent flow, the velocities fluctuate rapidly about their mean values. These fluctuations appear random in space and time and can only be described in statistical terms (*10*). A strongly flattened velocity profile, also called the block profile, is the characteristic of the turbulent flow. The turbulent velocity profile $v(r)$ cannot be treated analytically. One commonly used approximation leads to the so-called 1/7-law, based

1090-7807/01 $35.00

on the theory of Blasius and Prandtl (Eq. [4]) (*9*):

$$v(r) = v_{max} \cdot \left(1 - \frac{r}{r_0}\right)^{1/7}. \qquad [4]$$

This model describes the central portion of the flattened profile sufficiently well but not the transition toward laminar behavior observed near the wall. The flattening results from the tendency of the transverse velocity components to level out the velocity profile uniformly along the cross section.

The critical Reynolds number for Newtonian fluids in hydraulically smooth pipes is $Re_c = 2300$, independent of the fluid, where a pipe is called hydraulically smooth if the wall roughness does not extend beyond the region of laminar flow (*11, 12*). Hydraulic measurements confirm the different rheological behavior of blood from that of a Newtonian fluid. Blood documents a slightly reduced drag coefficient λ for turbulent blood flow relative to a water/glycerol mixture with comparable viscosity which represents the case of a Newtonian fluid (*13*). λ is given by the following relationship, which can be derived from Eq. [2] and comprises the friction effect in a pipe:

$$\Delta p = \lambda \cdot \frac{l}{d} \cdot \frac{p}{2}\bar{v}^2. \qquad [5]$$

Additionally a higher Re_c for blood of about 3000 compared to the value 2300 for the water/glycerol mixture was found (*13*). Here, the direct visualization of the flow profile by systematic variation of *Re* allows the comparison with existing fluid dynamic models and allows one to study the rheological behavior in detail.

NMR flow imaging was applied to blood flow, as the only method being able to visualize the flow pattern of such nontransparent fluids in a direct and noninvasive way. In the present work, one method for flow characterization was to measure the velocity profile using a spin-echo-based pulse sequence, containing flow-compensated slice selection in the axial direction (z), flow-compensated frequency encoding of the radial position (x), and the phase encoding of velocity in the main flow direction (z) using bipolar gradients (*14–16*) (Fig. 1a). The other method determines the statistical velocity distribution in the main flow direction, using pulsed field gradient (PFG) techniques with flow-compensated slice selection (*17*). This statistical velocity distribution represents the probability density of the averaged velocity over a defined observation time and corresponds to the displacement propagator so long as coherent and stationary flow conditions are given (*18, 19*) (Fig. 1b). Some basic experimental results are shown to understand these experiments in principle. In order to obtain the velocity profile, the NMR signal is measured in the k- versus q_v-space and subsequently Fourier transformed. The variables k and q_v are, respectively, the Fourier conjugate variables to the position and the averaged velocity:

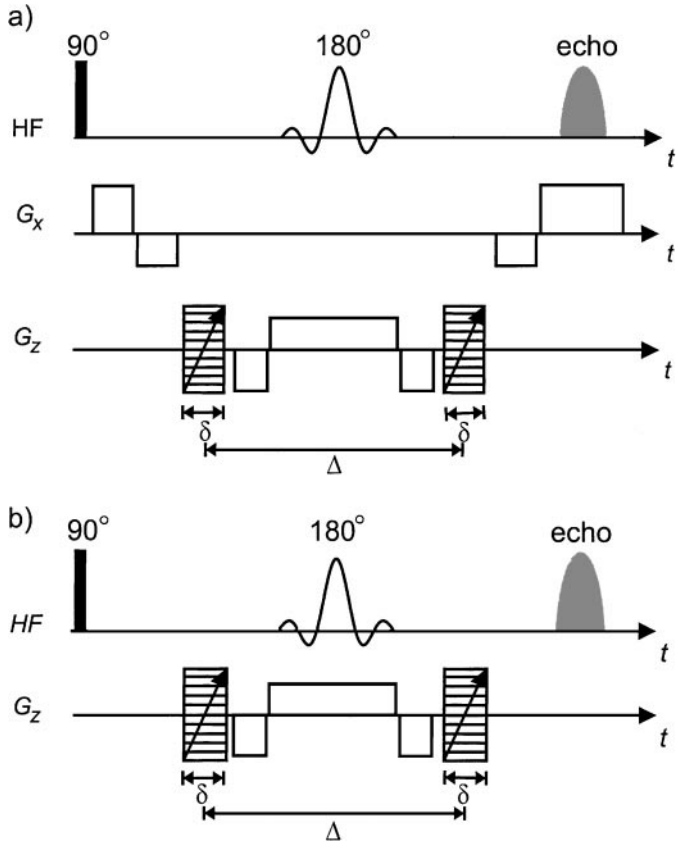

FIG. 1. (a) Spin-echo-based pulse sequence for measuring a velocity profile. This includes the velocity-compensated frequency encoding in the x (orthogonal to the pipe axis) direction, velocity-compensated slice selection, and bipolar phase encoding of the velocity in the z (parallel to the pipe axis) direction. This velocity compensation is fulfilled by calculating the appropriate gradient amplitudes and timing in between, so that the zeroth moment and the first moment of the gradient modulation funtion (*14, 15*) are both zero. The negative and positive gradients do not have the same amplitude. (b) PGSE (pulsed gradient spin echo) sequence with slice selection for measuring the velocity distribution.

$$\boldsymbol{k} = -(2\pi)^{-1} \cdot \gamma \cdot \int_0^t \boldsymbol{G}(t')\,dt',$$

$$\boldsymbol{q}_v = -(2\pi)^{-1} \cdot \gamma \cdot \int_0^t \boldsymbol{G}(t')t'\,dt. \qquad [6]$$

A perfectly laminar flow results in a parabolic velocity profile and a uniformly distributed velocity distribution of box shape (Fig. 2a). However, turbulent flow results in a flattened velocity profile, also called a block profile. A detailed pipe flow study of water by NMR imaging over a wide range of *Re* from 1200 to 9400 has already been reported in the literature (*20*) and demonstrated that NMR imaging is able to measure such kind of flattened profiles of turbulent flow (*17, 20*). The velocity distribution gets a characteristic shape, possessing a pronounced peak

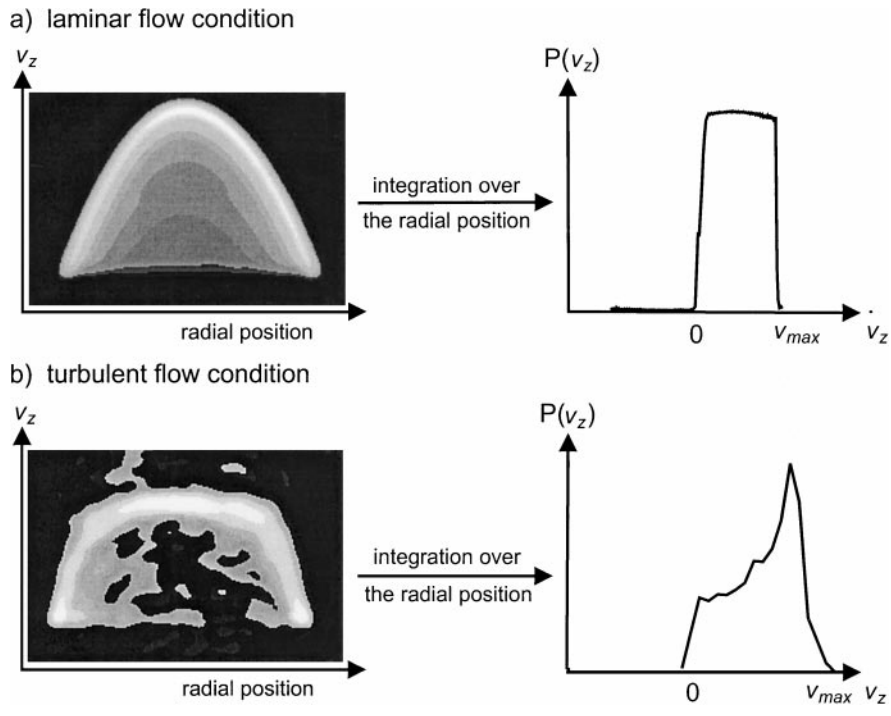

FIG. 2. The velocity profile and velocity distribution for (a) laminar pipe flow and (b) turbulent pipe flow, respectively. The experimental NMR data agree with the well-known behavior in pipe flow of Newtonian fluid.

at high velocities which means a larger fraction of spins moving at similar and large frontal velocity values, with only those water molecules in the vicinity of the tube wall having small velocities (*19*) (Fig. 2b). Thus, a distinction between laminar and turbulent flow can be made by investigating the shape of the velocity profile as well as the velocity distribution. Comparing these two types of representation, the velocity profile is easier to understand, because it gives a direct picture correlating position and velocity information. The shape of the statistical velocity distribution is an indirect image, but is more sensitive to the inhomogeneity in the flow behavior itself, like existing transverse components or pulsation, which changes its shape. While the deviation of the velocity profile from a parabola is difficult to quantify, a perfect box shape can be distinguished well from a distorted box.

A water/glycerol mixture and blood flowing through pipes of 7 and 1 mm inner diameter for *Re* numbers of 10 to 3500 were investigated as detailed before. The general flow behavior of a Newtonian fluid and the non-Newtonian fluid is compared for a wide range of flow velocities, and the transition from laminar to turbulent flow and the turbulent characteristics are the point of interest in this work.

EXPERIMENTAL

Experiments were performed on a horizontal 7-T, 200-mm bore magnet equipped with a Bruker DMX-300 spectrometer. In a mock loop, either a water/glycerol mixture, temperature controlled at 20°C, or fresh porcine blood[1] at 37°C was flowing in a Perspex pipe of 7 mm inner diameter. The water/glycerol was mixed with a volume fraction ratio of 40/100 resulting in a dynamic viscosity of 3.6 mPas, which matches the viscosity of blood. Porcine blood was used with a hematocrit value of 45% corresponding to physiological levels. To ensure a full polarization of all spins in the moving fluid between entering the magnetic field B_0 and reaching the resonator, the longitudinal relaxation time had to be reduced sufficiently. The water/glycerol mixture was doped with $CuSO_4$ to reduce T_1 to about 200 ms. For porcine blood, Magnevist (Schering, Berlin), a Gd-complex-based doping reagent commonly used in medical imaging applications, was added in a volume concentration of 0.05% in order to reduce the relaxation time, resulting in a similar T_1 value for the plasma and the erythrocytes of about 180 and 230 ms, respectively. Accordingly, the repetition time for all experiments was chosen to 500 ms, so that both components are relaxed after the recycling delay with a difference of less than 5%. The Perspex pipe was hydraulically smooth. The pipe length from the inlet to the point for measurements was chosen long enough to establish a stationary flow, and a disturbance in the form of a cross stick of 1 mm diameter was put in the inlet of the pipe in order to ensure defined conditions for the transition from laminar to turbulent flow (*13*). The velocity range was incremented from 0.05 to 1.75 m/s, corresponding to Reynolds numbers from 100 to

[1] Fresh porcine blood was treated with the anticoagulation additive heparin and the antibiotic refobacin.

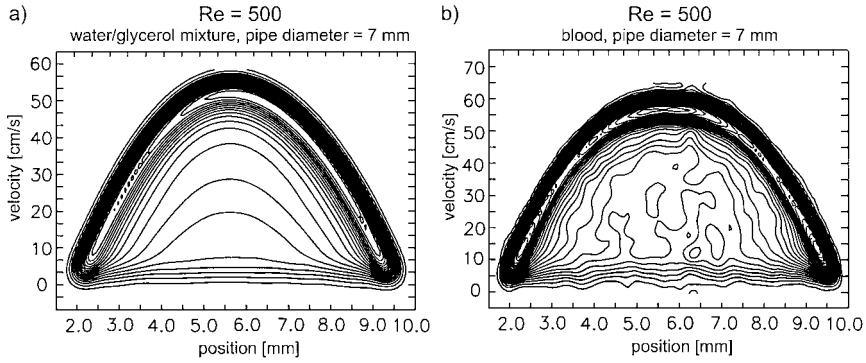

FIG. 3. The velocity profile of a water/glycerol mixture (a) and porcine blood (b) flowing in a pipe of 7 mm inner diameter at $Re = 500$. A perfect parabolic profile is presented in (a) as expected, whereas (b) shows deviation from it caused by the disturbing effect of the erythrocytes in blood.

3500. Under the same conditions, additional experiments were performed in a pipe with 1 mm inner diameter by varying flow velocities in the range of 1.7 to 0.03 m/s, which corresponds to the Reynolds numbers between 500 and 10. A centrifugal blood pump, BP80 (Biomedicus, Texas), was used which allows blood pumping for up to 12 h with minimum blood damage and works pulsation free. The flow rate was measured with an ultrasonic flowmeter which was calibrated before the measurements either for the water/glycerol mixture or for blood.

The velocity profiles were obtained using a conventional flow imaging spin-echo sequence as described above (Fig. 1a) with echo times between 4 and 7 ms and a slice thickness of 1.0 mm Because a wide range of velocity windows had to be covered by the measurements depending on the flow rates, it was indispensable to vary also the each time, not only the gradient amplitude. Acquiring one image took about 20 min, employing a repetition time of 500 ms and 8 averages. The velocity distribution was measured using a slice-selective PGSE sequence (Fig. 1b) with identical parameters. The flow encoding gradient was oriented parallel to the axial direction of the pipe which is defined as the z axis and the position encoding gradient was set perpendicular to it in the radial x direction. The flow encoding gradients were varied in 65 steps between $-G_{\max}$ and $+G_{\max}$, where $G_{\max}$ represents the maximum gradient strength in the z direction (Fig. 1b). The spatial resolution obtained was 78 μm/pixel for the 7-mm pipe and 23 μm/pixel for the 1-mm pipe.

RESULTS AND DISCUSSION

The velocity profiles of the water/glycerol mixture and blood, respectively, at a Reynolds number of 500 are presented in Fig. 3 as contour plots, connecting points with equal intensities. Remarkable are the perfectly arranged contour lines as found for the water/glycerol mixture compared to those of the blood profile. The shape of the profile of the blood velocity is still parabolic, but already at this low Reynolds number the deviation of the arrangements of the contour lines from the ideal case is clear, which indicates disturbances and transverse components of motion. Also apparent is the outer shape of the blood velocity profile, which is slightly flattened. This flattening effect was already observed for a transparent polymer solution of non-Newtonian behavior, employing Laser-Doppler velocimetry (*21*). The flattening of a profile can better be recognized by fitting the profile with a proper model function. The profile of the water/glycerol mixture is perfectly described by a parabolic function (Eq. [1]). On the other hand, as shown in Fig. 4 the blood profile differs slightly from a parabola.

We consider some rheological models with simple stress-rate-of-strain relations to model the measured blood flow behavior. The relationship between stress τ and rate of strain D is linear for a Newtonian fluid. So called power-law fluids show an empirical relationship between τ and D of the form

$$\tau = \eta \cdot D^s, \quad \text{where } s = 1 \text{ for a Newtonian fluid.} \qquad [7]$$

Bingham plastics possess the property that the friction between the sliding surface in the coupling makes extension impossible unless the force is greater than some frictional force. If the rate of extension beyond this value is proportional to the applied stress, the material is called an ideal Bingham plastic

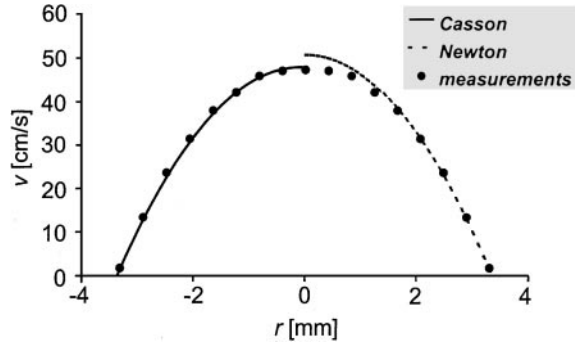

FIG. 4. Fit of a parabolic function (Hagen–Poiseuille, dotted line) and of Casson's model (solid line) to the velocity profile determined experimentally for porcine blood flowing in a pipe of 7 mm inner diameter at $Re = 500$.

and obeys the relationship

$$\tau = \tau_y + \eta \cdot D, \quad [8]$$

where τ_y is called the yield stress. Finally, the Casson model (*2*) is an empirical modification of the law for a nonideal Bingham plastic (Eq. [8]), given by

$$\sqrt{\tau} = \sqrt{\tau_y} + \eta \cdot \sqrt{D}. \quad [9]$$

Investigators have found that of the models discussed above, the two most successful ones are the power-law equation (Eq. [7]) and Casson's equation (Eq. [9]). Because evidently whole blood exhibits a yield stress, blood flow is best described as a Bingham plastic following the Casson equation. The constants τ_y and η were empirically determined by Whitmore to $\tau_y = 0.109$ and $\eta = 0.166$ (*22*):

$$\sqrt{\tau} = 0.33 + 0.166 \cdot \sqrt{D}. \quad [10]$$

The mathematical expression for the velocity profile resulting from Casson's model is

$$v(r) = \frac{\Delta p}{4 l \eta^2}\left(r_0^2 - r^2\right) - \frac{4}{3\eta^2}\left(\frac{\tau_y \cdot \Delta p}{2l}\right)^{1/2}\left(r_0^{3/2} - r^{3/2}\right) + \frac{\tau_y}{\eta^2}(r_0 - r), \quad [11]$$

where Δp is the pressure difference along the length of the tube l (*22*).

In Fig. 4 the blood profile was fitted with the parabolic function for Newtonian fluids (Eq. [1]) and with the profile following the Casson model of Whitmore (Eq. [11]). The blood velocity profile is described with good accuracy by this equation, which confirms on the one hand the Bingham character of blood possessing a yield stress, and on the other hand that blood does not behave like an idealized Bingham plastic but rather shows more complex behavior. One explanation why a fluid with particles does "not behave perfectly laminar" is the so-called Magnus effect (*23*). Because the shear stress is a function of the pipe radius, having its minimum in the center of the pipe and increasing linearly to the wall, particles in the current have the tendency to migrate toward the center of the pipe. As a consequence, the concentration of the cellular particles is higher toward the

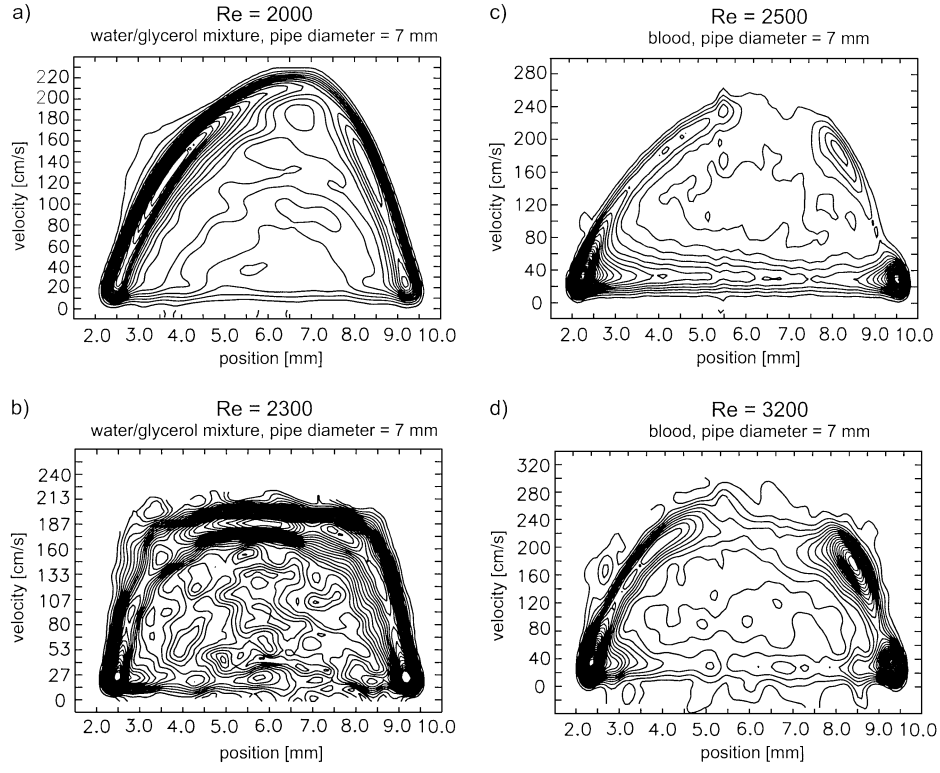

FIG. 5. The velocity profile of a water/glycerol mixture (a, b) and porcine blood (c, d) flowing in a pipe of 7 mm inner diameter at *Re* between 2000 and 3200. The transition from a more or less parabolic velocity profile (a) to a turbulent profile at $Re_c = 2300$ (b) can be seen. The critical *Re* number Re_c of blood is shifted toward a higher *Re* number of about 3200 (d). The velocity profile of blood shows neither at $Re < Re_c$ (c) a perfect parabola nor at $Re > Re_c$ (d) a perfect block profile which can be attributed to the suspension character of blood.

center of the pipe and therefore a stronger deviation from laminar behavior is expected here than in the vicinity of the wall. This effect is well shown in Fig. 3b and Fig. 4. The contour lines of the blood velocity profiles are more disturbed in the center already at low Reynolds number of about 500. Another effect, due to the particle migration caused by the Magnus effect, is a remaining liquid film at the pipe wall. This is similar to the laminar interfacial layer at the wall, which is always present in turbulent pipe flow. As shown in Fig. 3b, Fig. 5c, and Fig. 5d, the image intensity near the wall is much higher. This can be attributed to the fact that the fluid film at the pipe wall shows laminar behavior because the disturbing effect of the particles is missing, and so the NMR signal can be completely refocused. With increasing Reynolds number, the water/glycerol mixture possesses a transition from a laminar parabolic profile (Fig. 5a) to a flattened block profile (Fig. 5b) for turbulent flow at a Reynolds number approximately around 2300. This is in coincidence with values reported in (*11*). The somewhat disturbed but still parabolic blood profile keeps its shape above the $Re_c = 2300$ of the water/glycerol mixture and only at a Reynolds number of around 3200 a clearly flattened profile is measured. Still the shape of the profile is not as much flattened compared to that of the Newtonian fluid. All the effects of blood flow listed above agree with the theory that blood has always a disturbing and a damping character in its flow behavior, caused mainly by the fraction of the erythrocytes (*5*). The disturbing influence of the erythrocytes can be explained by the Magnus effect, resulting from the suspension character of blood, and the damping character can be attributed to the fact that erythrocytes are deformable and have viscoelastic characteristics. On the one hand, disturbances can be observed already at low Reynolds numbers around 500, while on the other hand, the parabolic shape is maintained for Reynolds numbers up to 3000. Due to the higher damping factor of blood, the transition

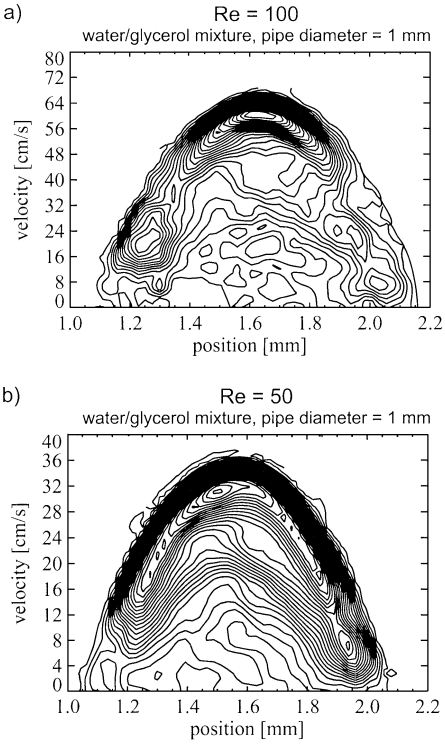

FIG. 6. The velocity profile of water at $Re = 100$ (a) and $Re = 50$ (b) flowing in a pipe of 1 mm diameter. The shape differs not very much from that in Fig. 3a and Fig. 4a at $Re = 500$ and $Re = 2000$, respectively, except for the lower signal-to-noise ratio.

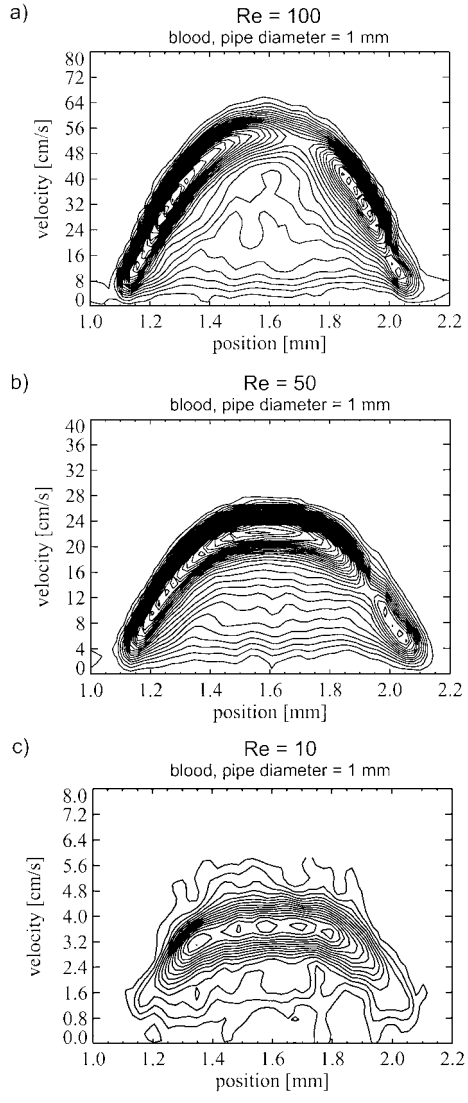

FIG. 7. The velocity profile of porcine blood at $Re = 100$ (a), $Re = 50$ (b), and $Re = 10$ (c) flowing in a pipe of 1 mm inner diameter. The profile at $Re = 100$ and $Re = 50$ is slightly flattened as already observed for all the blood profiles, whereas at $Re = 10$ a particularly strongly flattening is found. Even though the outer shape of this profile looks very much like that of a turbulent block profile, this feature can be explained with the rouleaux effect. The erythrocytes are supposed to stack to each other in parallel alignment in the shape of a pile and creep along the pipe, which results in an equalized front velocity over a broad cross section of the pipe.

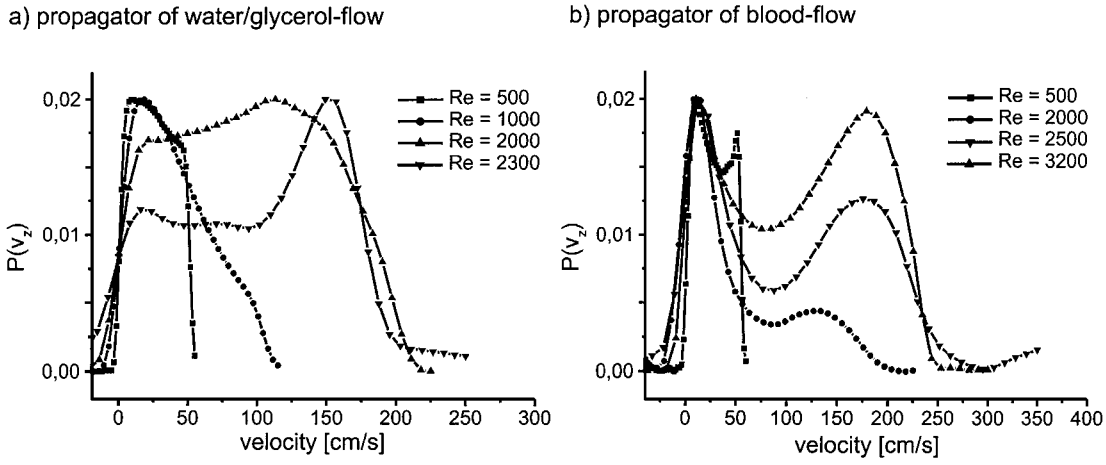

FIG. 8. Velocity distribution for a water/glycerol mixture (a) and porcine blood (b) flowing in a pipe of 7 mm inner diameter at *Re* between 500 and 3200. (a) The transition from a uniform distribution to a distribution with a higher intensity for the high velocity range is clearly visible. (b) The transition from laminar to turbulent flow cannot be definitely assigned. The profile at $Re = 500$ is more similar to a laminar velocity distribution but possesses an intensity peak, characterizing disturbances, whereas the profile at $Re = 3200$ rather resembles that of turbulent flow. The change from laminar to turbulent is a smooth transition different from that found for a Newtonian fluid. This feature very well represents the always existing disturbing and damping component in blood flow due to the presence of erythrocytes.

from laminar to turbulent flow is initiated at higher flow rates than for a Newtonian fluid.

Another series of experiments was performed in order[2] to observe blood flow at very low Reynolds numbers in a pipe of 1 mm diameter. Figures. 6 and 7 show the velocity profiles of blood compared to that of the water/glycerol mixture at Reynolds numbers of 100 and 50 and for blood flow also at *Re* number of 10. The velocity profiles of the water/glycerol mixture in a 1-mm tube at a Reynolds numbers of 100 and 50 in Fig. 6 do not differ very much from the velocity profile at $Re = 500$ in Fig. 3a or at $Re = 2000$ in Fig. 5a except for the lower signal-to-noise ratio as a consequence of the smaller probe volume. The behavior of blood flowing in a 1-mm tube at $Re = 100$ (Fig. 7) is similar to that of $Re = 500$ in a 7-mm pipe (Fig. 3b). The profile is of roughly parabolic shape but is clearly flattened compared to that of the water/glycerol mixture. By decreasing the Reynolds number, the flattening becomes more pronounced. The profile at $Re = 10$ appears similar to the turbulent block profile of blood at $Re = 3200$. This unusual behavior is based on the so-called rouleaux effect, found in very narrow blood vessels and under pathophysiological conditions.[2] According to theories (*24*, *25*), for very low shear rates erythrocytes have a tendency to aggregate and form piles, similar to coins arranging themselves to cash rolls, and move as a coherent structure. Therefore the blood flow behavior exhibits the block profile known from turbulent flow because the flowing particles are correlated in the form of a pile and the propagating velocity is almost equalized over the cross section.

[2] The rouleaux effect is often found with paraproteinaemia, caused by the pathological proliferation of a clone of immunoglobulin producing atypical lymphocytes.

An alternative approach for investigating the flow behavior is to measure the velocity distribution. In Fig. 8a the velocity distribution of the water/glycerol mixture is shown. One can clearly see how the more or less uniform distribution at $Re = 500$ suddenly turns to a completely different shape at $Re = 2300$ which features a very high intensity for the fastest particles resulting in an intensity peak on the right-hand side. The velocity profile at $Re = 500$ in Fig. 3a looks perfectly parabolic, but the propagator has a nonperfect box shape in Fig. 8a. This demonstrates the higher sensitivity of the velocity propagator to deviations from ideal laminar flow than the velocity profile. If the pipe is horizontally balanced and a pulsation-free pump is used, a perfect box can be measured as demonstrated in Fig. 2. In our case, a slight deviation from the idealized condition is present, which can only be observed in the velocity distribution presentation. The velocity distribution of blood in Fig. 8b also shows the development to a more pronounced pattern for turbulent flow at $Re = 3200$. A remarkable fact in Fig. 8b is that at all Reynolds numbers from 500 to 3200 an intensity peak on the right-hand side of the profile can be observed. This can be interpreted in the same way as the always existing flattening of the velocity profile of blood caused by the disturbing characteristics of the erythrocytes induced by the Magnus effect. Flattening of the profile means that fluid particles in the broad flowing front tend to have equally high velocities, resulting in an intensity peak at the high velocity region of the distribution. The flattening of the velocity profile can only be discussed if various model functions are compared to the experimental velocity profile, but an intensity peak of a velocity distribution can be clearly observed without comparison to models. This is one of the advantages of this velocity-distribution presentation although not giving direct velocity information correlated to the position.

CONCLUSIONS

In a pipe flow study, the particular flow characteristics of blood were shown for a wide range of flow velocities and Reynolds numbers. We conclude that blood exhibits a higher flow instability already at low Reynolds numbers but also a higher damping capacity for turbulent excitations. These effects can very likely be attributed to the high concentration (40–50%) of erythrocytes in the suspension. Erythrocytes as particles flowing within the plasma always have a disturbing character to flow. The migration of the erythrocytes toward the center of the pipe due to the Magnus effect was observed in blood flow, confirming the suspension character of blood. On the basis of erythrocytes being ductile and elastic, they are responsible for the damping of the blood flow at high Reynolds numbers. This is the explanation why the critical Reynolds number Re_c of blood was observed at higher values of about 3000, compared to the Re_c of the water/glycerol mixture as a Newtonian fluid. This is in agreement with hydraulic measurements reported in the literature (*13*). One peculiarity observed for blood flow is the flattening of the velocity profile, similar to the behavior in turbulent flow, also at very low Reynolds numbers of about 10. This can be explained by the so-called rouleaux effect, where the erythrocytes are stacked in parallel alignment in the shape of a pile and joined together creep along the pipe. This behavior results in plug flow with an almost homogeneous front velocity. These first NMR imaging investigations of blood flow given some detailed insight to the special rheological behavior of blood. Although the observations are obtained for the simplest geometry under nonpulsatile, thus unphysiological, conditions, the basic understanding of simple blood flow is fundamental to biomechanical applications, and may further be useful for physiological investigations of blood flow, typically the study of vessels with arteriosclerosis.

ACKNOWLEDGMENTS

The work group of Dr. H. Reul at the HIA led by Professor G. Rau provided us with porcine blood and blood flow equipment. We are grateful to Dr. S. Stapf for editorial elaboration and discussions. The cooperation in the experimental setup with Dr. P Blümler is acknowledged. We thank K. Kupferschläger, M. Adams, G. Schröder, and P. Schwindke for setting up the pump station.

REFERENCES

1. P. L. Altman and D. S. Dittmer, "Blood and Other Body Fluids," 3rd ed., Fed. Am. Soc. Exp. Biol., Bethesda, Maryland (1971).
2. S. A. Berger, W. Goldsmith, and E. R. Levis, "Introduction to Bioengineering," Oxford Univ. Press, Oxford (1996).
3. J. R. Singer, Blood flow rates by nuclear magnetic resonance measurements, *Science* **130,** 1652 (1959).
4. E. F. Blick, H. N. Sabbah, and P. D. Stein, Red blood cells and turbulences, *in* "Proceedings, 4th Biannual Symposium on Turbulences," p. 116 (1975).
5. W. A. Munter and P. D. Stein, Newtonian behaviour of blood at high rates of shear, *Biorheology* **10,** 501 (1973).
6. W. A. Munter and P. D. Stein, Turbulent blood flow and the effect of erythrocytes, *Cardiovasc. Res.*, 338 (1974).
7. J. Apel, H. Reul, and G. Rau, *Int. J. Artif. Organs* **21,** 646 (1998).
8. H. Reul, "Advances in Cardiovascular Engineering: Design, Development and Testing of Blood Pumps," (N. H. C. Hwang, *et al*., Eds.), Plenum, New York (1992).
9. H. Schlichting and K. Gersten, "Boundary Layer Theory," 8th revised and enlarged ed., Springer-Verlag, Berlin (2000).
10. S. P. Sutera and J. H. Joist, "Haematological Effects of Turbulent Blood: Thrombosis, Embolism and Bleeding," ICR Pub. London (1992).
11. O. Reynolds, *Philos. Trans. R. Soc. London B. Biol. Sci.* **174,** 935 (1883).
12. L. Schiller, Untersuchungen über laminare und turbulente Strömung, *Forsch. Ing.-Wes.*, 428 (1922).
13. O. Marseille, "Entwicklungs- und Bewertungsverfahren für Rotationspumpen," Dissertation, RWTH, Aachen, Germany (2001).
14. J. M. Pope and S. Yao, *Concepts Magn. Reson.* **5,** 281 (1993).
15. S. Laukemper-Ostendorf, K. Rombach, P. Blümler, and B. Blümich, "3D NMR—Imaging of Flow in Stationary Systems," Bruker Note (1998).
16. B. Blümich, "NMR Imaging for Materials," Oxford Science Publications (2000).
17. P. T. Callaghan, "Principles of Nuclear Magnetic Resonance Microscopy," Clarendon Press, Oxford (1991).
18. J. Kärger, H. Pfeifer, and W. Heink, *Adv. Magn. Reson.* **12,** 1 (1988).
19. S. Han, and B. Blümich, *Appl. Magn. Reson.* **18,** 101 (2000).
20. T. Q. Li, J. D. Seymour, R. L. Powell, K. L. McCarthy, L. Ödberg, and M. J. McCarthy, *Magn. Reson. Imaging* **12,** 923 (1994).
21. D. Liepsch, *Biorheology* **23,** 395 (1986).
22. R. L. Whitmore, "Rheology of the Circulation," Pergamon Press, Oxford (1968).
23. D. Leighton and A. Acrivos, *J. Fluid Mech.* **181,** 415 (1987).
24. G. R Cokelet, E. W. Merrill, E. R. Gilliland, and H. Shin, *Trans. Soc. Rheol.* **7,** 303 (1963).
25. T. Shiga, K. Imaizumi, N. Harada, and M. Sekiya, *Am. J. Physiol.* **245**(2), 252 (1983).